

## A note on flexible hydropower and security of supply: Spain beyond 2020

Luis M<sup>a</sup> Abadie <sup>a</sup>, José M. Chamorro <sup>b\*</sup>, Sébastien Huclin <sup>a</sup>, Dirk-Jan van de Ven <sup>a</sup>

<sup>a</sup> Basque Centre for Climate Change (BC3), Sede Building 1, 1st floor,  
Scientific Campus, University of the Basque Country UPV/EHU, 48940 Leioa, Spain. *E-mails:*  
[lm.abadie@bc3research.org](mailto:lm.abadie@bc3research.org), [sebastien.huclin@bc3research.org](mailto:sebastien.huclin@bc3research.org), [dj.vandeven@bc3research.org](mailto:dj.vandeven@bc3research.org)

<sup>b</sup> University of the Basque Country UPV/EHU, Dpt. Financial Economics II,  
and Institute of Public Economics, Av. Lehendakari Aguirre 83, 48015 Bilbao, Spain.

*E-mail:* [jm.chamorro@ehu.eus](mailto:jm.chamorro@ehu.eus)

\* Corresponding author.

October 2<sup>nd</sup> 2019

### ABSTRACT

Generation adequacy is a key ingredient to security of electricity supply (SoS). Some national plans envisage a future decrease in the number of coal-fired stations and an increase in renewable installed capacity. This forecast, along with the future reduction of nuclear capacity, will lead to a combination of less baseload plants and sizeable intermittent generation. Hence there is a risk that supply will be unable to meet demand and generation adequacy will suffer.

We assess how the flexible management of hydro resources can alleviate this risk by adjusting power generation to peak demand. Indeed there is empirical evidence that they are positively correlated. We compute this correlation in the case of Spain (an ‘electric island’). Besides, hydro plants operate in combination with other non-dispatchable technologies within the system. Therefore, we also take their hourly seasonality into account. Next we run a Monte Carlo simulation to derive the risk profile of several adequacy metrics in the coming decades. Our results show that flexible hydro generation certainly mitigates the risk but is insufficient to bring an adequate level of SoS when the enhanced renewable capacity goes hand in hand with a decreased baseload capacity. The risk further decreases after accounting for seasonal non-dispatchable generation, yet it still looms large. These results can be important for policy makers, system operators, and power companies when analyzing investments in renewable energy with a long lifespan.

*Keywords:* security of electricity supply, generation adequacy, hydro stations, uncertainty, Monte Carlo, lost load.

### 1 INTRODUCTION

As the overall demand for electricity is anticipated to increase in the future, security of electricity supply (henceforth SoS) is eliciting ever more attention from all the stakeholders involved. It seems fair to claim that there is hardly a widely accepted definition of SoS. Nonetheless, a common thread arises from the different versions, namely the ability of power supply to meet effective demand on a continuous basis. In a sense this is a ‘narrow’ definition since power demand and supply do not operate in a vacuum. [1] goes beyond it by encompassing also environmental and societal concerns. This makes sense because SoS is affected by a number of factors, among them technology, markets, politics, and the environment.

The power supply in particular is a complex chain that is naturally exposed to a number of risks and uncertainties. As a demarcation criterion, the probabilities and/or impacts of the former can be more reliably computed than those of the latter. Sources of uncertainty are typically addressed by means of scenario analysis. Instead, regarding risks, the standard practice is to define and compute a number of risk metrics. This said, supply is only 50 percent of the story. [2] defines system adequacy as the existence within a system of sufficient generation and transmission capacity to meet the load, whether under normal or unusual conditions. It subsequently introduces different approaches to measure adequacy and a list of related metrics.

[3] develop a stochastic model that explicitly matches power demand and supply (if possible). From this interplay it is possible to assess generation adequacy by means of several metrics that account for different attributes of potential supply shortfalls. Next they demonstrate the model by example.

1  
2  
3 Specifically, they look at Spain (an ‘electric island’ right now and in the near future at least) beyond the year  
4 2020. Monte Carlo (MC) simulation allows them derive the risk profile of several key variables. Taken  
5 together they characterize the risk profile to SoS in great detail.

6 In the end, [3] simulate the performance of the Spanish peninsular generating system under ten  
7 different scenarios. Regarding the installed generation capacities from 2020 through 2050, they basically  
8 draw on [4]. Importantly, [3] assume that coal-fired and nuclear stations are kept constant from 2017 to  
9 2020 but decrease significantly in 2030 and completely cease to operate from 2040 onwards; natural gas  
10 plants, instead, are assumed to remain constant at their 2017 level through 2050. Unlike thermal stations,  
11 renewable power technologies grow in all of the scenarios, be it either slower or faster depending on the  
12 growth of power demand (either 1.36% or 1.72%). According to their results [3], the system’s adequacy  
13 worsens in 2020 and does so dramatically in 2040 and 2050, when coal and nuclear stations are completely  
14 replaced by renewable plants.

15  
16 The earlier results in [3] consider all power technologies as feeding their potential output in the  
17 system irrespective of demand; this general rule applies to hydro power in particular too. Because of the  
18 earth’s gravitational field there is energy stored in the water that flows in rivers from upstream regions  
19 toward the sea. So-called diversion or run-of-river hydropower refers to extracting a portion of the energy  
20 contained in flowing water itself to produce electricity. Another possibility is to use the potential energy  
21 contained by a dam structure for the same purpose; this is frequently called impoundment hydropower; [5].  
22 Importantly, this type of facilities can regulate the flow to be turbined at any precise time. Despite the  
23 differences between both types, [3] consider all hydropower plants (HPPs) as a whole. Thus, the results in  
24 [3] take monthly seasonality of hydro’s load factor into account, but there is no room for strategic  
25 management of hydro plants (i.e. no aim at maximizing profits by producing more electricity at demand  
26 peaks within the month).<sup>1</sup> By no means this is exclusive of [3]; indeed it seems to be the usual practice. For  
27 example, [2] presents the findings from an empirical analysis on adequacy metrics and standards adopted in  
28 Europe. From the research conducted via public sources, one of the general conclusions drawn reads as  
29 follows: *“In no case was it mentioned how the operation of hydropower plants with reservoirs is  
30 considered. In countries with medium or high participation of hydropower in the generation mix, this factor  
31 is crucial for system security. In fact, in some of these countries, a dry year may be the most stressful  
32 situation in relation to generation adequacy. The use of historical series of generation data would ignore  
33 the possibility of operating reservoirs in a conservative manner, in order to increase generation adequacy  
34 (or equivalently, to reduce the risk of load shedding)”*. In view of this, the EC urges to consider at least the  
35 probabilistic characterization of a number of factors, among them: *“Hydroelectric energy availability  
36 depends on the reservoir operation strategies established by the owners of plants”*.

37  
38  
39 Hydropower plants with reservoirs can in principle serve several purposes, for example irrigation  
40 needs or flooding control. HPPs can be managed as SoS devices also. They are normally designed for  
41 generation during peak hours.<sup>2</sup> Further, some HPPs are equipped with reversible turbines or separate  
42 generating and pumping equipment (so-called pumped storage hydropower).<sup>3</sup> They enable the system to  
43 pump water (using electricity) from a lower reservoir up to a higher one when power demand (and  
44 presumably price) is low; when demand (price) increases, the flow is reversed. This ‘load leveling’ is a  
45 widespread type of load management; [7]. ‘Ramping and load following’ are other types of load  
46

47  
48  
49  
50  
51  
52  
53  
54  
55  
56  
57  
58  
59  
60  
61  
62  
63  
64  
65  
<sup>1</sup> Note that deciding when it will be more profitable to produce electricity is no easy task. At one level, suppliers draw on limited hydro energy resources available. On the other hand, future inflows are uncertain and there is a risk of spillage. According to [6], generators try to hedge against risk and are usually conservative. For example, they generally opt for deploying limited water resources when prices are moderately high, instead of waiting for a possible (uncertain) scarcity of generating resources (when the peak price would be very high) in the future.

<sup>2</sup> The flexibility of hydro reservoirs is often seen as the perfect complement to a system dominated by intermittent renewable sources; [7], [8]. [9] and [10] even claim that a system based on only wind, water and solar power could serve 100% of energy purposes by 2050 in a reliable and affordable way. However, this claim has received various critiques, e.g. that these authors are too optimistic about the balancing role of hydropower [11].

<sup>3</sup> Pumped hydro storage is the major energy storage technology. It accounts for 96% of the world storage capacity [9]; compressed air, batteries, thermal and flywheel energy storage play very minor roles. [7] and [12] highlight some of its applications (along with some barriers to its development), such as offsetting the intermittence of renewable sources and providing ancillary services to the power system (e.g. voltage regulation).

1  
2  
3 management, in which energy storage is used to assist generation to follow the load changes. In this regard,  
4 [13] point out that the business case for price arbitrage has vanished partly owing to the injection of  
5 subsidized renewable electricity during peak demand periods. To avoid becoming uneconomic, pumped  
6 storage stations have to find additional sources of revenue. [14] consider the Austrian-German spot power  
7 market and the Austrian balancing energy market through the years 2012-2015. They find that earnings  
8 from the latter may exceed those from the former many times over.

9  
10 The empirical evidence shows that hydro operation does follow demand to some extent.  
11 Specifically, these stations generate relatively more power during peak hours and less in non-peak ones. On  
12 the other hand, these plants operate alongside other (non-dispatchable) technologies in a system. For  
13 example, wind energy blows during the night, when power demand is relatively lower; pump stations can  
14 avoid wasting this energy by storing it. Consequently, a detailed analysis of the contribution of hydropower  
15 to SoS calls for taking due consideration of non-dispatchable sources.<sup>4</sup> This note is an extension of [3] on at  
16 least three accounts. First, it aims to account for that positive correlation between maximum hourly  
17 demand and hydropower generation to check the potential of flexible management to reinforce SoS.  
18 Second, we disaggregate hydro stations between run-of-river (RoR) stations and the remainder (non-RoR)  
19 stations.; this way we want to account for the different degree of freedom between the two types when it  
20 comes to flexible management. Third, we also consider the hourly seasonality in generation from  
21 non-dispatchable technologies during peak hours. In addition, for these three reasons, now the numerical  
22 application (via MC simulation) gets more complex than in [3]. Thus, relative to [3], this paper contributes  
23 in scope, method, and policy implications. To our knowledge, no other paper on applied SoS adequacy  
24 metrics addresses the role of hydro-based generation in mitigating power supply shortfalls or the  
25 potential of seasonal non-dispatchable generation in meeting peak demands (let alone in the way we do).

26  
27 In 2017 hydro stations (including pumped storage) represented about 20% of the total capacity  
28 installed in the Spanish mainland system (20,331 MW out of 99,311 MW); in terms of power generation,  
29 they provided around 8.3% of the total. Would the flexibility of hydropower alleviate estimates of supply  
30 shortages in [3]? How effective is it in enhancing SoS in mainland Spain? In the same vein, does  
31 consideration of seasonal non-dispatchable generation contribute to quell SoS concerns? If so, to what  
32 extent? According to our results, the positive correlation between hourly peak demand and flexible  
33 hydropower's generation significantly tempers the severity of the negative impacts of demand surges. The  
34 situation further improves when hourly seasonality of non-dispatchable generation is considered.  
35 Nonetheless, the expected energy not served (*EENS*) jumps above historical levels in 2030 and runs into the  
36 tens of thousands megawatts-hour thereafter. The issue is of interest not only to Spanish consumers and  
37 utilities, but also to other stakeholders involved in the construction of the European internal power market.  
38 Further, climate change might exacerbate the high variability that characterizes renewable energy sources  
39 in general and hydro power generation in particular; [15].

40  
41 The remainder of the paper is organized as follows. Section 2 extends the model in [3] to account  
42 for the flexible operation of hydropower stations in mainland Spain and also the seasonal pattern of  
43 renewable generation. The resulting impact on the adequacy metrics is analyzed in Section 3. Section 4  
44 concludes.

## 45 46 **2 ACCOUNTING FOR HYDROPOWER FLEXIBILITY AND SEASONAL** 47 **NON-DISPATCHABLE GENERATION**

### 48 49 **2.1. Model extension**

50  
51 [3] propose a model for evaluating generation adequacy in the long run from the viewpoint of the  
52 facilities installed. Even though power demand can be relatively predictable at this time scale, unexpected  
53 peak loads can certainly occur also in the short run; [16].

54 Given their focus on generation adequacy they naturally pay special attention to peak demand.  
55 Typically demand surges are short lived. Publicly available records on power demand stretch back over  
56

57  
58 <sup>4</sup> We thank an anonymous reviewer for bringing this issue to our attention.  
59  
60  
61  
62  
63  
64  
65

many years, even decades. Unfortunately, however, their sample data on peak demand are very limited. They resort to an indirect approach that relies on yearly data; specifically, they relate the hourly peak demand in a future year ( $\tilde{q}$ , in MWh) to the annual demand in that year ( $\tilde{Q}$ , in MWh):

$$\ln \tilde{q} = \alpha + \beta \times \ln \tilde{Q} + \tilde{e}; \quad (1)$$

$\tilde{e}$  stands for an independent and identically distributed random shock. By assumption, the natural logarithm of maximum hourly demand every year follows a Normal distribution with average  $\alpha + \beta \times E[\ln Q]$  (where  $E$  denotes the mathematical expectation operator) and standard deviation equal to the standard error of the regression. This is a stochastic equation: though the average growth rate of  $\tilde{q}$  depends on the average growth rate of  $\tilde{Q}$ , by its very nature  $\tilde{q}$  will grow above it some times, and below it some others.

Regarding power supply, they distinguish two groups of generation technologies. The first group comprises thermal technologies: coal ( $c$ ), natural gas ( $g$ ), and nuclear ( $n$ ). Each station has a particular installed capacity (MW) and availability rate (%). Availability is represented by a binary variable ( $A$ ). A particular station  $i$  of type  $j \in \{c, g, n\}$  is in service for a fraction  $\Lambda_j^i$  of the year (it can either actually run or remain idle depending on power demand); it is out of service for another fraction  $1 - \Lambda_j^i$  (because of failures and maintenance works):

$$A_j^i = \begin{cases} 0, \text{'off' state with probability } 1 - \Lambda_j^i \\ 1, \text{'on' state with probability } \Lambda_j^i \end{cases}. \quad (2)$$

The second group of generation technologies includes hydro, wind, solar (both photovoltaic and thermal), cogeneration, and others. The time series of power produced/consumed by these stations subsumes both the usual pattern of failures and their intermittent nature. Consequently, [3] adopt the load factor for describing these intermittent technologies and assume that these show a stochastic behavior with both the monthly average and the volatility changing from one month to another.<sup>5</sup> They adopt the Weibull distribution to describe this variable across all of the technologies in this group.<sup>6</sup> The probability density function of the load factor ( $x$ ) is:

$$f(x) = \begin{cases} \frac{k}{\lambda} \left(\frac{x}{\lambda}\right)^{k-1} e^{-\left(\frac{x}{\lambda}\right)^k} & \text{if } x \geq 0 \\ 0 & \text{if } x < 0 \end{cases}, \quad (3)$$

where  $\lambda \in (0, +\infty)$  is the scale parameter and  $k \in (0, +\infty)$  is the shape parameter. The cumulative density function is:

$$F(x) = \begin{cases} 1 - e^{-\left(\frac{x}{\lambda}\right)^k} & \text{if } x \geq 0 \\ 0 & \text{if } x < 0 \end{cases}. \quad (4)$$

The average and the variance are given by:

$$\mu = \lambda \Gamma\left(1 + \frac{1}{k}\right), \quad (5)$$

$$\sigma^2 = \lambda^2 \left[ \Gamma\left(1 + \frac{2}{k}\right) - \left(\Gamma\left(1 + \frac{1}{k}\right)\right)^2 \right], \quad (6)$$

where  $\Gamma$  denotes the gamma function.

This pattern for the generation technologies in the second group applies to hydropower generation. In this sense, Eqs. (3)-(6) may be a reasonable approach as long as [3] consider hydro generation as a single power source or technology. Nonetheless, unlike [3], here we are going to disaggregate hydro stations between RoR stations and non-RoR stations. The former are relatively more dependent on natural (re)charge and less amenable to strategic management. Consequently, we are going to estimate an independent Weibull distribution for RoR stations according to Eqs. (3)-(4). Hence we can get numerical estimates of the average ( $\mu_R$ ) and the variance ( $\sigma_R$ ) following Eqs. (5)-(6); the subindex  $R$  refers to these particular stations. Non-RoR stations include conventional reservoirs (of seasonal, annual or pluriannual regulation) and pumped storage stations (of daily, weekly or seasonal cycle). In principle they are more amenable to strategic operation and lend themselves more easily to track demand surges. Again, we assume that the load factor of these stations can be characterized by a Weibull distribution, Eqs. (3)-(4), with

<sup>5</sup> Multiplying the load factor times the installed capacity allows derive samples of monthly power generation later on.

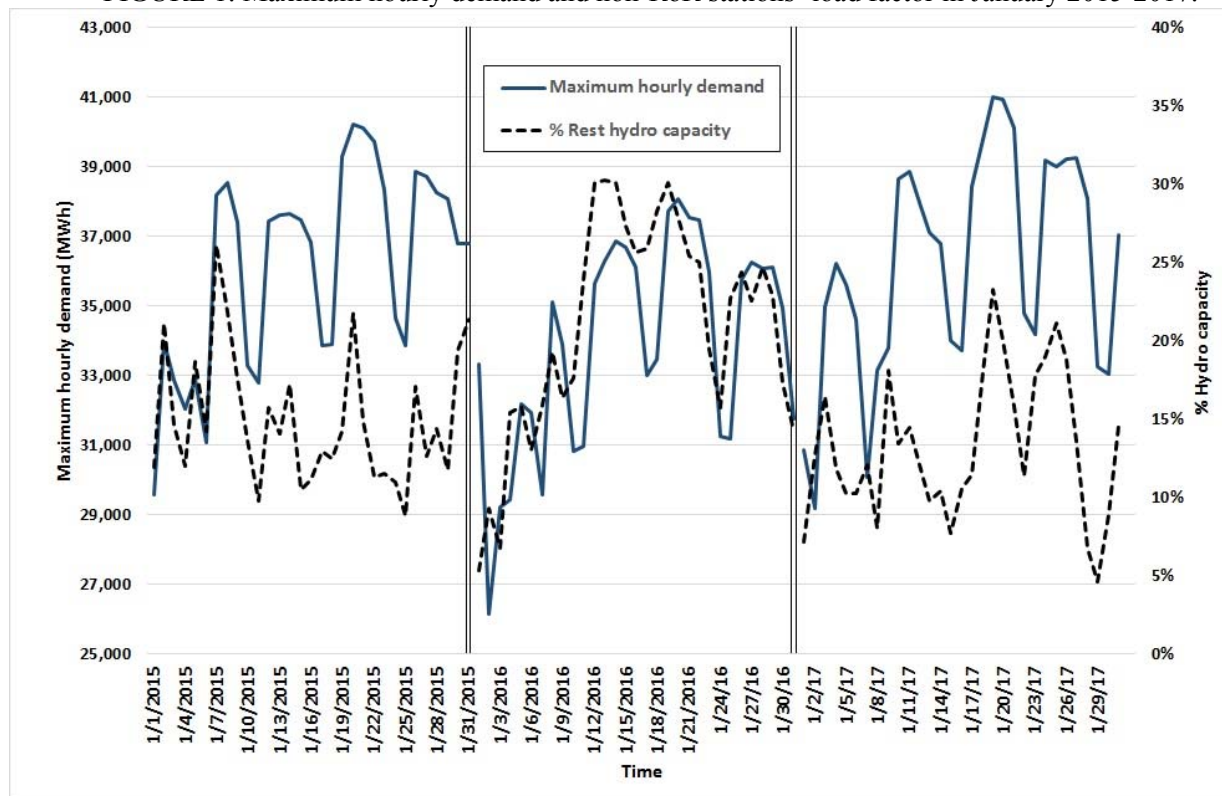
<sup>6</sup> Note that the Weibull distribution does not admit negative values, which is just right when dealing with load factors.

1  
2  
3 associated average ( $\mu_P$ ) and ( $\sigma_P$ ) according to Eqs. (5)-(6); we adopt the subindex  $P$  for these hydro plants.  
4 Unlike RoR, however, the Weibull distribution for non-RoR stations is going to be correlated with peak  
5 demand.

6 Now the information available differs from data in [3] in three key respects: (a) we know the  
7 maximum hourly demand in each single day of the years 2015, 2016, and 2017, i.e. we have 365+366+365  
8 = 1,096 data; (b) we know hydro-based power generation during the hours of peak demand over those  
9 years; (c) we also have hydro-based installed capacity every day (from linear interpolation between  
10 monthly values); the combined information of (b) and (c) allows computing this technology's load factor on  
11 a daily basis. Figure 1 displays the time path of hourly peak demand (a) along with non-RoR stations' load  
12 factor in January over the sample period. It suggests that these series are positively correlated. As a matter  
13 of fact, the correlation coefficient is 0.256 (the last column in Table 3 below shows the coefficient in the  
14 other months). In June it reaches the lowest value, close to zero. The upper bound is almost 45% and applies  
15 in March. The main driver behind this comovement is that power utilities manage these plants in an  
16 opportunistic or strategic way since peak demands are usually associated with higher prices (indeed hydro  
17 is the 'marginal' technology on the wholesale power market in many instances).  
18  
19  
20  
21  
22

23  
24  
25  
26  
27  
28  
29  
30  
31  
32  
33  
34  
35  
36  
37  
38  
39  
40  
41  
42  
43  
44  
45  
46  
47  
48  
49  
50  
51  
52  
53  
54  
55  
56  
57  
58  
59  
60  
61  
62  
63  
64  
65

FIGURE 1: Maximum hourly demand and non-RoR stations' load factor in January 2015-2017.



Later on we will run a number of simulations (note that the main adequacy metrics in [3] draw on a probabilistic MC approach). Regarding RoR stations, to this end we will use the average ( $\mu_R$ ) and the variance ( $\sigma_R$ ) estimated according to Eqs. (5)-(6). However, in the case of non-RoR stations we will need to generate correlated samples. We start by deriving two independent samples  $x_P^*$  and  $x_D^*$  of non-RoR stations' load factor and hourly peak demand (note the subindex  $D$ ). In a second step we normalise each

series by subtracting its average and dividing by its volatility. Thus we obtain two independent, normalised samples  $x_P$  and  $x_D$  of the load factor and peak demand, respectively. In a third step we construct correlated samples,  $v_D$  and  $v_P$ , according to the scheme:

$$v_D = x_D; v_P = x_D\rho + x_P\sqrt{1 - \rho^2}, \quad (7)$$

where  $\rho$  stands for the correlation coefficient between the two daily series.

## 2.2. Parameter estimation in addressing correlation

Our sample data include daily power generation and installed capacity for the two types of hydro stations. Data on these variables (b) and (c) allow computing separate, specific load factors on a daily basis. Next we arrange all of the daily load factors by month. Thus, there are 31+31+31=93 daily factors in January, 28+29+28=85 factors in February, and so on. With the daily factors in any single month we estimate a Weibull distribution for that particular month, i.e. we estimate the scale ( $\lambda$ ) and shape ( $k$ ) parameters for every month.

### 2.2.1. Run-of-river stations

The left block in Table 1 shows the monthly estimates of the Weibull parameters for RoR stations along with their 95 percent confidence intervals. For the scale parameter ( $\lambda$ ) the intervals are rather narrow. The difference between the upper and lower bounds is minimum in March (4.07%) and maximum in May (10.7%). Instead, the intervals are wider for the shape parameter ( $k$ ). The difference ranges between 33.1% (October) and 40.2% (January).

The next step is to substitute the monthly values of  $\lambda$  and  $k$  in Eqs. (5)-(6) to compute the monthly average and standard deviation of RoR stations' load factor; see the right block in Table 1. Looking at  $\mu_R$ , the mean is highest in March; henceforth it declines consistently until October and then rises. Similarly, the highest volatility  $\sigma_R$  is reached in April and the lowest one in September. Therefore, through the three sample years, the extreme values of the mean and the volatility are rather contemporaneous. The maximum generation takes place from February to May. In 2017 the installed capacity of RoR stations was 2,104 MW [17]; see Table A1 in the Appendix.

| Month     | Scale ( $\lambda$ ) |             | Shape ( $k$ ) |              | Average | Volatility |
|-----------|---------------------|-------------|---------------|--------------|---------|------------|
|           | Value               | 95% int.    | Value         | 95% int.     | $\mu_R$ | $\sigma_R$ |
| January   | 0.520               | 0.499—0.542 | 5.163         | 4.360—6.114  | 0.479   | 0.106      |
| February  | 0.668               | 0.651—0.684 | 9.178         | 7.766—10.846 | 0.633   | 0.083      |
| March     | 0.734               | 0.717—0.751 | 9.330         | 8.019—10.854 | 0.696   | 0.089      |
| April     | 0.715               | 0.680—0.750 | 4.424         | 3.767—5.195  | 0.652   | 0.167      |
| May       | 0.659               | 0.626—0.693 | 4.241         | 3.624—4.961  | 0.599   | 0.160      |
| June      | 0.531               | 0.507—0.555 | 4.825         | 4.153—5.606  | 0.486   | 0.115      |
| July      | 0.412               | 0.398—0.426 | 6.364         | 5.482—7.386  | 0.384   | 0.070      |
| August    | 0.358               | 0.347—0.370 | 6.680         | 5.759—7.747  | 0.335   | 0.059      |
| September | 0.303               | 0.293—0.313 | 6.418         | 5.500—7.487  | 0.282   | 0.051      |
| October   | 0.270               | 0.258—0.281 | 4.962         | 4.301—5.723  | 0.248   | 0.057      |
| November  | 0.369               | 0.351—0.387 | 4.457         | 3.802—5.224  | 0.337   | 0.086      |
| December  | 0.407               | 0.390—0.424 | 5.156         | 4.454—5.968  | 0.375   | 0.083      |

### 2.2.2. Non-RoR stations

For the rest of hydro (non-RoR) stations, as stated earlier, we assume that the Weibull distribution describing their load factor is correlated with peak demand; see Figure 1. In 2017 the capacity installed amounted to 18,227 MW; see Table A1 in the Appendix. We display the Weibull parameter estimates in Table 2. Again, the confidence intervals are thinner for the scale parameter than for the shape parameter.

Hence we further compute the average and the volatility of the load factor ( $\mu_P$ ,  $\sigma_P$ ) by means of Eqs. (5)-(6).

| Month     | Scale ( $\lambda$ ) |             | Shape ( $k$ ) |             | Average | Volatility |
|-----------|---------------------|-------------|---------------|-------------|---------|------------|
|           | Value               | 95% int.    | Value         | 95% int.    | $\mu_P$ | $\sigma_P$ |
| January   | 0.406               | 0.385—0.427 | 4.113         | 3.513—4.813 | 0.368   | 0.101      |
| February  | 0.447               | 0.421—0.475 | 3.692         | 3.080—4.425 | 0.404   | 0.122      |
| March     | 0.470               | 0.448—0.492 | 4.584         | 3.903—5.383 | 0.430   | 0.107      |
| April     | 0.374               | 0.343—0.406 | 2.585         | 2.198—3.039 | 0.332   | 0.138      |
| May       | 0.355               | 0.325—0.386 | 2.492         | 2.117—2.933 | 0.315   | 0.135      |
| June      | 0.285               | 0.264—0.306 | 2.951         | 2.500—3.483 | 0.254   | 0.094      |
| July      | 0.251               | 0.230—0.272 | 2.535         | 2.153—2.982 | 0.223   | 0.094      |
| August    | 0.225               | 0.208—0.243 | 2.837         | 2.418—3.327 | 0.201   | 0.077      |
| September | 0.222               | 0.207—0.237 | 3.146         | 2.678—3.694 | 0.199   | 0.069      |
| October   | 0.252               | 0.232—0.271 | 2.758         | 2.336—3.256 | 0.224   | 0.088      |
| November  | 0.262               | 0.239—0.288 | 2.343         | 1.981—2.770 | 0.233   | 0.105      |
| December  | 0.266               | 0.244—0.289 | 2.598         | 2.202—3.065 | 0.236   | 0.098      |

Table 3 shows the descriptive statistics of hourly peak demand and further information about the correlation with power generation from non-RoR stations.<sup>7</sup> The latter sheds light on the statistical significance and accuracy of the monthly estimates. We start from the standard (Pearson) formula (thus assuming a linear relationship between both variables). As a safeguard against sampling error we conduct a test. The null hypothesis is  $\rho = 0$ . The alternative hypothesis is  $\rho \neq 0$  (which requires a two-tail test). The  $t$ -test for the correlation observed is:

$$t = \frac{\rho\sqrt{n-2}}{\sqrt{1-\rho^2}}, \quad (8)$$

where  $n$  stands for the number of observations; this  $t$ -test has  $n-2$  degrees of freedom. As for the confidence interval we first turn the observed correlation into Fisher's transform:

$$z' = \frac{1}{2} \ln \frac{1+\rho}{1-\rho}. \quad (9)$$

Hence the interval for the  $z'$  transform is computed as:

$$IC(z') = \left[ z' - 1.96 \frac{1}{\sqrt{n-3}}; z' + 1.96 \frac{1}{\sqrt{n-3}} \right]. \quad (10)$$

And the resulting interval for the correlation observed is calculated as:

$$IC(\rho) = \left[ \frac{\exp\left(2\left(z' - \frac{1.96}{\sqrt{n-3}}\right)\right) - 1}{\exp\left(2\left(z' - \frac{1.96}{\sqrt{n-3}}\right)\right) + 1}; \frac{\exp\left(2\left(z' + \frac{1.96}{\sqrt{n-3}}\right)\right) - 1}{\exp\left(2\left(z' + \frac{1.96}{\sqrt{n-3}}\right)\right) + 1} \right]. \quad (11)$$

The information above allows assess the robustness of our numerical estimates.

| Month    | Hourly peak demand |            | Correlation Coefficient |        |            |                |
|----------|--------------------|------------|-------------------------|--------|------------|----------------|
|          | $\mu_D$            | $\sigma_D$ | # Obs.                  | $\rho$ | $p$ -value | 95% conf. int. |
| January  | 35,424             | 3,207      | 93                      | 0.256  | 0.0132     | 0.055—0.437    |
| February | 35,280             | 2,528      | 85                      | 0.381  | 0.0003     | 0.183—0.550    |

<sup>7</sup> We thank an anonymous referee for raising this point.

|           |        |       |    |        |        |              |
|-----------|--------|-------|----|--------|--------|--------------|
| March     | 33,340 | 2,563 | 93 | 0.449  | 0.0000 | 0.270—0.598  |
| April     | 30,715 | 2,338 | 90 | 0.326  | 0.0017 | 0.128—0.499  |
| May       | 30,572 | 2,251 | 93 | 0.101  | 0.3364 | -0.105—0.299 |
| June      | 33,048 | 2,953 | 90 | -0.012 | 0.9115 | -0.219—0.196 |
| July      | 35,290 | 3,158 | 93 | 0.369  | 0.0003 | 0.179—0.533  |
| August    | 33,186 | 2,954 | 93 | 0.215  | 0.0382 | 0.012—0.401  |
| September | 32,236 | 2,766 | 90 | 0.194  | 0.0674 | -0.014—0.386 |
| October   | 31,087 | 2,335 | 93 | 0.179  | 0.0869 | -0.026—0.369 |
| November  | 33,174 | 2,903 | 90 | 0.152  | 0.1514 | -0.057—0.348 |
| December  | 33,654 | 2,998 | 93 | 0.101  | 0.3370 | -0.105—0.299 |

We are going to simulate a Weibull distribution 50,000 times each month using the parameter values of  $\lambda$  and  $k$  and then compute the average load factor and its volatility. Provided the latter closely mirror those derived from our sample data, the numerical estimates of the MC-based adequacy metrics can be considered reliable. Table A2 in the Appendix shows the results from both the sample data and the simulation runs in each month. The (negligible) differences observed can be attributed to the limited number of runs and the very nature of random numbers.

Regarding the maximum hourly demand, we resort to Eq.(1). As in [3], we take random samples for the shock term and shift the maximum demand curve in 2017 accordingly. Specifically we use 50,000 simulation runs (i.e. years, each comprising 365 days). We group them by month and compute the monthly average and volatility,  $\mu_D$  and  $\sigma_D$ , respectively; see the left block columns in Table 3. Peak demand surges typically in January (35,424 MWh) and July (35,290); these months are also the most volatile ones (3,207 MWh and 3,158, respectively).

The right block in Table 3 proves the importance of extending [3] along the lines drawn in this note. To begin with, at the yearly level (i.e. neglecting differences across months) the correlation between non-RoR stations' load factor and hourly peak demand is 0.214 (statistically different from zero at the 5% confidence level). The analysis on a monthly basis shows that, for most of the year, there is a mild correlation. It ranges from about 0 to 25% in eight out of twelve months, slightly alleviating power supply shortages (the computation draws on all the daily values of both variables in any single month). Nonetheless, the flexibility advantage of hydropower gets larger in months with a high load factor (January to April), with the correlation coefficient rising up to 45%; this suggests that higher water levels in reservoirs do allow a more flexible and strategic management of those reservoirs; [18], [19]. Just half of the monthly estimates of  $\rho$  are statistically different from zero (again, at the 5% confidence level). Interestingly, they are significant from January to April along with July and August, precisely the months when the coefficient reaches its highest values. This said, we can also observe that the confidence intervals are wide, the upper bound being several times higher than the lower one on many occasions. This confirms the usefulness of accounting for the seasonal behavior of the correlation between non-RoR's load factor and peak demand, and of using monthly parameters in this analysis.

Monthly differences in correlation can be traced back to several issues.<sup>8</sup> On the supply side, within non-RoR stations there are HPPs with reservoirs (installed capacity 11,900 MW) and pumped storage stations (6,327 MW). Spain has 20 pumped storage plants.<sup>9</sup> They were commissioned through the 20<sup>th</sup> century mainly to address rainfall variability. So-called Hydrographic Confederations rule the basins; they are legally above hydropower operators since they set limits on the use of water. From this perspective, somehow there is an upper bound on power generation from non-RoR stations which is affected by both

<sup>8</sup> We thank an anonymous referee once more for bringing this issue to our attention.

<sup>9</sup> They can be further subdivided into two types: pure or closed-loop (where water is first pumped to an upper reservoir and then released to generate power) and mixed or open-loop (when there are water contributions from rivers). Pure pumped storage accounts for 53% of the total (3,337 MW) while mixed pumped storage takes the remaining 47%.



1  
2  
3 actual rainfall and water needs. The so-called ‘*hydropower potential*’ measures the maximum amount of  
4 electricity that could be theoretically produced from the water contributions during a particular period of  
5 time after subtracting the water diverted for irrigation or other uses different from power generation. Table  
6 A3 and Figure A1 in the Appendix show that the highest hydropower potentials are available during the  
7 first three or four months of the year. They subsequently decline through summer and start rising in autumn.

8 At the same time, power demand also plays a role here; it changes seasonally over time (Table A3  
9 and Figure A1 in the Appendix). The average peak demand in particular is highest in January and July  
10 (Table 3) followed by February (which lags close behind, with 35,280 MWh). In general, the first months of  
11 the year tend to be also the months when the correlation between peak demand and hydro’s load factor is  
12 relatively higher (as shown in Table 3); this also applies to July (maybe in an effort to make ends meet).

13 Anyway, a cautionary note seems in order. Water reserves at the end of 2017 were at their lowest  
14 level on record (starting 1990); [20]. Hydro-based generation decreased almost in half with respect to 2016,  
15 and reached its lowest value since 2005. Hydro was the third power generation source in 2016 but dropped  
16 to the sixth in 2017. The drought in 2017 dragged renewable generation down from 40.3% of total in 2016  
17 to 33.7% in 2017. This episode attests to the high variability of renewable resources, both at yearly and  
18 monthly levels (for one, hydro-based generation contributed 26% of total power in May 2016 but 10.1% in  
19 May 2017, its lowest level on record).

20 Annual variability certainly complicates drawing conclusions from just three years of observations.  
21 Yet a fact speaks for itself: in 2017 the average contribution of pure pumped storage to power generation  
22 was just 0.9%; nonetheless, it jumped to 6.7% in the day of peak demand (January 25th); [20]. This fact  
23 highlights its role in addressing SoS concerns.  
24

### 25 26 27 **2.3. Parameter estimation in addressing seasonality**

28 Our initial model does not account for any hourly seasonality. Note, however, that we do not use the  
29 24 hourly demands in any single day, but only the maximum hourly demand in that day. We proceed as  
30 follows.

31 We consider the twelve months of 2017, our base year. Every day in every month has a maximum  
32 hourly demand at a particular time. We take each month in isolation and identify the most frequent hour at  
33 which the maximum hourly demand takes place. Thus, in the case of January, the typical hour with  
34 maximum demand is 21:00; instead, in July it is 14:00.

35 We have hourly power generation by all of the non-dispatchable technologies other than non-RoR  
36 (i.e. RoR, wind, solar, cogeneration, and others) from 2015 through 2018, i.e. four years. Now, let’s think of  
37 a particular renewable technology, say wind, and a particular month, say January. There are four such  
38 months in the sample, each running from day 1 to day 31. We thus have  $4 \times 31 = 124$  January days; we adopt  
39 the sub-index  $k$  for each one of them, with  $k = 1, 2, \dots, 124$ . On the other hand, each day comprises 24 hours,  
40 denoted by sub-index  $i$ , with  $i = 1, 2, \dots, 24$ . Therefore, we have 142 observations for hour 1 in January,  
41 another 142 observations for hour 2 in January, 142 observations for hour 3 in January, and so on until hour  
42 24 in January.  
43

44 Initially we compute the hourly average generation in each day ( $\mu_k$ ) summing up its 24 hourly  
45 levels and then dividing by 24. Next, we divide each of these 24 hourly levels in day  $k$  by the hourly average  
46 that day ( $\mu_k$ ) just calculated. This way we derive a series of seasonal factors for each hour, with each series  
47 comprising 124 terms. We denote each factor by  $\varphi_{ik}$  (again, with  $i = 1, 2, \dots, 24$  and  $k = 1, 2, \dots, 124$ ).  
48 Drawing on the 124 values for hour  $i$ , the  $i$ -th seasonal factor for wind in January is just their average:

$$49 \quad \varphi_i = \frac{1}{124} \sum_{k=1}^{124} \varphi_{i,k}, \text{ where } i = 1, 2, \dots, 24. \quad (12)$$

50 Thus we get a series of 24 factors ( $\varphi_i$ , with  $i = 1, 2, \dots, 24$ ), one for each hour of the day in January; they can  
51 be interpreted as representing hourly seasonality (in generation from wind). Some of them are higher than 1,  
52 and some others are lower than 1; they sum to 24:

$$53 \quad \sum_{i=1}^{24} \varphi_i = 24. \quad (13)$$

54 Henceforth, we follow this procedure: we simulate the daily average generation in any single  
55 January day from wind ( $\mu$ ). Then we use the above factors  $\varphi_i$  (based on empirical/historical evidence) to  
56  
57  
58  
59  
60  
61  
62  
63  
64  
65

account for the hourly variability in generation from wind (note that they in turn depend on the empirical averages  $\mu_k$ ). Specifically, since we have 24 factors  $\phi_i$ , we compute 24 hourly generation levels from wind in that January day. This way we hope to address the issue raised by the Reviewer (as we interpret it: potential seasonalities at the hourly level).

Needless to say, the same procedure is applied every other month, from February to December. It is also applied across non-dispatchable technologies. The only exception is non-RoR, whose hourly seasonality was already taken into account through its correlation with hourly peak demand. The aim is to compare the ensuing results with those when seasonality is left aside.

Table 4 below shows the most frequent hour of maximum demand in each month. Power demand reaches its hourly maximum around 21:00 in seven months. The other months, instead, the maximum is reached around 14:00. Table 4 also displays the factor  $\phi_i$  that applies to each non-dispatchable technology in that particular hour. A value above 1.0 means that the technology is operating “above daily average” at that precise time (e.g. wind at 21:00 in January); a value below 1.0 means the opposite (e.g. solar at 21:00 in January).

| Month     | Hour  | Wind   | Solar  | Cogen. | Others | RoR    | Non-RoR |
|-----------|-------|--------|--------|--------|--------|--------|---------|
| January   | 21:00 | 1.0340 | 0.0944 | 1.0222 | 1.0239 | 1.1139 | 1.8184  |
| February  | 21:00 | 1.0548 | 0.1386 | 1.0244 | 1.0268 | 1.0866 | 1.6418  |
| March     | 21:00 | 1.0512 | 0.2592 | 1.0171 | 1.0198 | 1.0663 | 1.5909  |
| April     | 22:00 | 1.1077 | 0.2443 | 1.0190 | 1.0210 | 1.0539 | 1.5965  |
| May       | 13:00 | 0.8423 | 2.2985 | 0.9981 | 1.0007 | 1.0342 | 1.2429  |
| June      | 14:00 | 0.7797 | 2.2280 | 0.9921 | 0.9951 | 1.0577 | 1.4104  |
| July      | 14:00 | 0.7297 | 2.1776 | 0.9933 | 0.9969 | 1.1121 | 1.5841  |
| August    | 14:00 | 0.7389 | 2.4004 | 0.9962 | 0.9978 | 1.1165 | 1.5479  |
| September | 14:00 | 0.7468 | 2.6408 | 0.9960 | 0.9983 | 1.0737 | 1.2829  |
| October   | 21:00 | 1.0779 | 0.2027 | 1.0090 | 1.0117 | 1.1255 | 2.2618  |
| November  | 21:00 | 1.0330 | 0.0932 | 1.0089 | 1.0135 | 1.1290 | 1.9737  |
| December  | 21:00 | 1.0162 | 0.0758 | 1.0072 | 1.0119 | 1.1241 | 1.9565  |

Note: A factor above (respectively, below) 1.0 means power generation above (resp., below.) daily average.

### 3 FLEXIBILITY, SEASONALITY, AND ADEQUACY METRICS

Here we assess the impacts of both factors on the adequacy metrics for mainland Spain and how they compare to the results in [3]. We do it sequentially: we start considering flexibility in isolation, and then we add seasonal non-dispatchable generation on top of it.

#### 3.1. Flexible hydropower

First, we illustrate how the flexible management of hydro stations alleviates supply shortages in mainland Spain. Regarding power demand, as explained in [3], maximum hourly demand in a year is regressed on yearly demand as shown in Eq. (1) from 1990 through 2017. The ordinary least squares regression analysis yields  $\alpha = -7.24270$  ( $t$ -ratio = -10.82),  $\beta = 0.924459$  ( $t$ -ratio = 26.45), and adjusted  $R$ -squared of 0.976980; the standard error of the regression is 0.034453. Hence, starting from the demand level in 2017 and assuming both a particular growth rate (e.g. 1.36%) and number of years ahead (say, 13) we can derive a forecast for total demand in, say, the year 2030. Substituting the resulting level in the regression equation we derive the (log) average peak demand in that year. Next we can simulate the maximum hourly demand in each day of the year 2030 in mainland Spain. Any particular simulation run (out of 50,000) yields a particular peak demand in that year. We compute the difference between this simulated peak demand and the actual peak demand in 2017. In order to get the hourly peak demand in 2030

on a daily basis we shift vertically the whole demand curve in 2017 downwards/upwards by this amount.

As for mainland power supply, Table A1 in the Appendix shows the generation mix by technology at year-end 2017. It is exactly the same as in [3]. The only difference is that now we separate hydro capacity between RoR and non-RoR technologies. Specifically, RoR capacity is assumed to remain constant through the time horizon considered (up to 2050) at 2,104 MW. Instead, non-RoR capacity starts from 18,227 MW in 2017 and grows more or less over time according to the assumed yearly growth of power demand (whether 1.36% or 1.73%). Regarding thermal plants, we perform 50,000 simulation runs of their available capacity in each month. As for non-thermal technologies, we derive 50,000 random samples of their load factor in each month; the two types of hydro stations are considered separately (just like any other technology). Then we compute the combined power generation from both thermal and non-thermal stations. The resulting level is multiplied by a factor of 0.9809 (the availability rate of Spanish power grid).

As already mentioned, [4] consider two scenarios of future demand growth: 1.36% and 1.73% per year. [3] stick with these two demand scenarios, denoted  $D_1$  and  $D_2$ , respectively. Concerning supply, depending on the assumed growth rate of demand, they adopt different installed capacities for each technology in the coming decades. Thermal stations in particular show the same path in all the scenarios: coal-fired and nuclear stations remain constant from 2017 to 2020 but decrease significantly in 2030 and completely cease to operate from 2040 onwards; natural gas plants, instead, are assumed to remain constant at their 2017 level through 2050. Non-thermal power technologies undergo weaker or stronger growth according to demand growth. [3] denote these generation systems by  $S_1$  and  $S_2$ , assumed to match demands  $D_1$  and  $D_2$ , respectively; see Table A1 in the Appendix. In the end, [3] simulate the performance of the Spanish peninsular generating system in ten different scenarios. After matching the earlier two parks  $S_1$  and  $S_2$  with demands  $D_1$  and  $D_2$ , they are subsequently combined with a flat future demand ( $D$ ). These four scenarios  $[(S_1, D_1), (S_2, D_2), (S_1, D), (S_2, D)]$  are then followed by another four in which the base demands are lowered by 5%  $[(S_1, D_1^-), (S_2, D_2^-), (S_1, D^-), (S_2, D^-)]$ . Finally, [3] take the scenarios  $[(S_1, D_1^-), (S_2, D_2^-)]$  and compare them with two other scenarios where gas-fired generation capacity is increased since 2030 through 2050, denoted  $[(S_1^+, D_1^-), (S_2^+, D_2^-)]$ .

We focus on the last two specific cases, namely  $[(S_1^+, D_1^-), (S_2^+, D_2^-)]$ . In them annual demand grows (on average) at 1.36% or 1.73% (denoted  $D_1$  and  $D_2$ , respectively) and so does hourly peak demand (on average), but the associated hourly peak demand levels are cut by 5% if necessary from 2030 onwards; we refer to them as ‘shaved’ demand ( $D_1^-$  or  $D_2^-$ ). At the same time, natural gas-fired generation capacity grows by 3,000 MW every decade; we refer to this as ‘enhanced’ supply ( $S_1^+$  or  $S_2^+$ ). This corresponds to the lower block of Table 7 in [3]; the upper part of Table 5 here replicates it for convenience; it represents inflexible hydropower generation. Remember that these demand growth scenarios envisage a wide deployment of renewable sources of electricity in [3]. The middle block in Table 5, instead, displays the adequacy metrics under flexible management of hydropower.

As expected, the positive correlation between hourly peak demand and flexible hydro’s load factor tempers the severity of the negative impacts of demand surges. Table 6 shows the decrease that applies to each probabilistic metrics in each year considered. For instance, in 2020 the percentage change in *EENS* with respect to inflexible management equals  $[(2/48) - 1] \times 100 = -95.8\%$  (under  $D_1^-$ ) or  $[(3/85) - 1] \times 100 = -96.5\%$  (under  $D_2^-$ ). This is obviously a dramatic reduction in the supply shortfall. Yet the impact fades over time as demand keeps on growing (whether at 1.36% or 1.73% per year) despite the broad deployment of renewable sources; by the end of the time horizon the drop in *EENS* is close to 60% or 55%, respectively. The same dynamics applies to the other adequacy metrics, whether we look at their average values or the 95 percentiles. Interestingly, the probability that the peak load will exceed available generation, *LOLP*, is basically unaffected in 2040 and 2050.

|    | 2017    | 2020    | 2030    | 2040    | 2050    | 2020    | 2030    | 2040    | 2050    |
|----|---------|---------|---------|---------|---------|---------|---------|---------|---------|
| AD | 253,082 | 263,621 | 302,026 | 346,026 | 396,436 | 266,564 | 316,909 | 376,762 | 447,920 |

|             |        |  |         |          |          |  |         |          |           |
|-------------|--------|--|---------|----------|----------|--|---------|----------|-----------|
| MHD         | 42,398 | 44,013   | 47,365  | 53,661   | 60,801   | 44,463   | 49,502  | 58,023   | 68,023    |
| AC          | 99,311 | 113,232  | 121,430 | 126,948  | 141,648  | 110,832  | 126,630 | 140,648  | 168,548   |
|             |        | <i>Inflexible hydro generation (<math>S_1^+, D_1^-</math>)</i>   |         |          |          | <i>Inflexible hydro generation (<math>S_2^+, D_2^-</math>)</i>   |         |          |           |
| <i>EENS</i> | 23     | 48   | 1,415   | 151,248  | 317,338  | 85   | 3,485   | 258,069  | 547,173   |
| <i>E95</i>  | 0      | 0  | 4,814   | 483,212  | 874,788  | 0  | 21,963  | 736,823  | 1,342,998 |
| <i>LOLE</i> | 1.44   | 2.54   | 53.01   | 2,945.50 | 4,980.68 | 4.27   | 115.01  | 4,219.63 | 6,614.56  |
| <i>L95</i>  | 0      | 0  | 420     | 7,500    | 10,920   | 0  | 840     | 9,600    | 12,780    |
| <i>LOLP</i> | 0.55   | 0.88   | 10.40   | 93.72    | 98.24    | 1.36   | 18.21   | 97.33    | 99.43     |
| <i>RM</i>   | 1.34   | 1.57   | 1.56    | 1.37     | 1.33     | 1.49   | 1.56    | 1.42     | 1.48      |
|             |        | <i>Flexible hydro generation (<math>S_1^+, D_1^-</math>)</i>     |         |          |          | <i>Flexible hydro generation (<math>S_2^+, D_2^-</math>)</i>     |         |          |           |
| <i>EENS</i> | 23     | 2  | 98      | 46,124   | 124,546  | 3  | 301     | 92,784   | 247,847   |
| <i>E95</i>  | 0      | 0  | 0       | 171,687  | 387,350  | 0  | 847     | 307,807  | 667,387   |
| <i>LOLE</i> | 1.44   | 0.10   | 4.80    | 1,218.85 | 2,617.18 | 0.21   | 13.12   | 2,046.40 | 3,993.92  |
| <i>L95</i>  | 0      | 0  | 0       | 3,660    | 6,540    | 0  | 60      | 5,400    | 8,520     |
| <i>LOLP</i> | 0.55   | 0.12   | 3.35    | 92.01    | 98.43    | 0.24   | 7.45    | 97.08    | 99.69     |
| <i>RM</i>   | 1.34   | 1.57   | 1.56    | 1.37     | 1.33     | 1.49   | 1.56    | 1.42     | 1.48      |
|             |        | <i>Flexibility &amp; Seasonality (<math>S_1^+, D_1^-</math>)</i> |         |          |          | <i>Flexibility &amp; Seasonality (<math>S_2^+, D_2^-</math>)</i> |         |          |           |
| <i>EENS</i> | 23     | 0.15   | 77.96   | 30,987   | 79,401   | 2.77   | 234.32  | 57,855   | 151,234   |
| <i>E95</i>  | 0      | 0  | 0       | 125,788  | 265,549  | 0  | 354.16  | 212,929  | 446,637   |
| <i>LOLE</i> | 1.44   | 0.01   | 3.75    | 773.91   | 1,577    | 0.16   | 10.06   | 1,197    | 2,339     |
| <i>L95</i>  | 0      | 0  | 0       | 2,400    | 4,080    | 0  | 60      | 3,300    | 5,220     |
| <i>LOLP</i> | 0.55   | 0.01   | 2.74    | 85.25    | 95.54    | 0.19   | 5.90    | 91.75    | 98.34     |
| <i>RM</i>   | 1.34   | 1.57   | 1.56    | 1.37     | 1.33     | 1.49   | 1.56    | 1.42     | 1.48      |

|             | Demand growth: +1.36% |         |        |        | Demand growth: +1.73% |        |        |        |
|-------------|-----------------------|---------|--------|--------|-----------------------|--------|--------|--------|
|             | 2020                  | 2030    | 2040   | 2050   | 2020                  | 2030   | 2040   | 2050   |
| <i>EENS</i> | -95.8%                | -93.1%  | -69.5% | -60.8% | -96.5%                | -91.4% | -64.0% | -54.7% |
| <i>E95</i>  | -                     | -100.0% | -64.5% | -55.7% | -                     | -96.1% | -58.2% | -50.3% |
| <i>LOLE</i> | -96.1%                | -90.9%  | -58.6% | -47.5% | -95.1%                | -88.6% | -51.5% | -39.6% |
| <i>L95</i>  | -                     | -100.0% | -51.2% | -40.1% | -                     | -92.9% | -43.8% | -33.3% |
| <i>LOLP</i> | -86.4%                | -67.8%  | -1.8%  | 0.2%   | -82.4%                | -59.1% | -0.3%  | 0.3%   |

In sum, the possibility of shortages still looms large in the long term and remains worrying. For one, *EENS* amounted to 23 MWh in 2017; according to our results, it falls to just 2 or 3 in 2020 but jumps to a few hundred in 2030 and runs into the hundreds of thousands afterward.

To some extent, the contribution of flexible hydropower management to SoS reflects the particular operation of pure pumped storage (PHES) plants in Spain. Figure A2 in the Appendix displays their actual operation profile over the period 2014-2018. Even though their aggregate installed capacity amounts to 3,337 MW, their usual net output is quite far from operation at full capacity. This fact may be attributed to a number of factors, such as profitability of hydro plants (see footnote 1), constraints due to reservoir volume or reservoir seasonal constraints [8].

### 3.2. Flexible hydropower and seasonal renewable generation

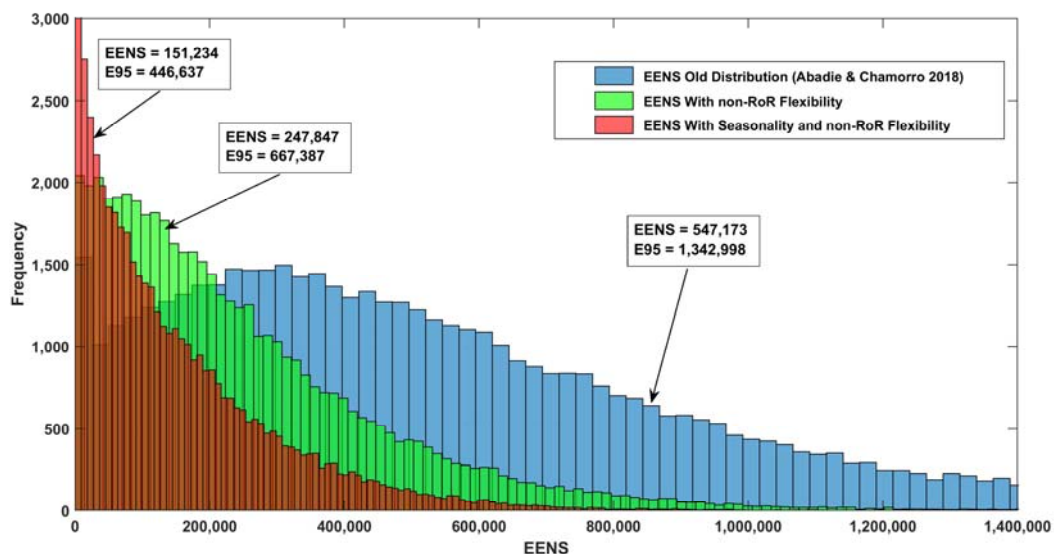
Now we assess the impact of seasonality in combination with hydropower flexibility. For this purpose, we focus on the lower block in Table 5 and compare it with the central one (flexible hydropower generation). From a cursory look it is clear that accounting for hourly seasonality does alleviate SoS

concerns. Table 7 shows that, in 2020, *EENS* drops dramatically under slow demand growth,  $[(0.15/2)-1]\times 100 = -92.3\%$ , but much less under faster growth,  $[(2.77/3)-1]\times 100 = -7.8\%$  (probably, some values close to zero in that year have an oversized impact on the percentage changes). From then on, the size of the reduction grows with the passage of time (and further deployment of renewables), ranging between 20% and 40%, which is a significant improvement. The 95<sup>th</sup> percentile (*E95*) decreases too, thus improving the severity of the shortfalls. The average number of hours in a given year with *EENS* occurrence (*LOLE*) falls a bit more than *EENS*; the same applies to its 95<sup>th</sup> percentile (*L95*) with respect to *E95*. Unlike these metrics, the probability that the peak load will exceed available generation (*LOLP*) does not drop so much; worse still, the decrease gets smaller over time, leaving *LOLP* almost unaffected by 2050.

|             | Demand growth: +1.36% |       |       |       | Demand growth: +1.73% |       |       |       |
|-------------|-----------------------|-------|-------|-------|-----------------------|-------|-------|-------|
|             | 2020                  | 2030  | 2040  | 2050  | 2020                  | 2030  | 2040  | 2050  |
| <i>EENS</i> | -92.3                 | -20.5 | -32.8 | -36.2 | -7.8                  | -22.2 | -37.6 | -39.0 |
| <i>E95</i>  | —                     | —     | -26.7 | -31.4 | —                     | -58.2 | -30.8 | -33.1 |
| <i>LOLE</i> | -88.0                 | -21.8 | -36.5 | -39.7 | -22.9                 | -23.3 | -41.5 | -41.4 |
| <i>L95</i>  | —                     | —     | -34.4 | -37.6 | —                     | 0.0   | -38.9 | -38.7 |
| <i>LOLP</i> | -88.3                 | -18.1 | -7.3  | -2.9  | -22.5                 | -20.9 | -5.5  | -1.4  |

Figure 2 displays the probability distribution of *EENS* for the year 2050 under the second demand growth scenario ( $D_2$ ) in the three settings: the default situation (as in [3], i.e. without taking correlation and seasonality into account), with correlation (i.e. flexible hydropower management), and with both correlation and seasonality. As we move from the first setting to the second one there is a massive displacement of the probability mass towards the left. As observed in Table 6, when hydro operators follow peak demand the *EENS* is cut almost by 55 % while its 95<sup>th</sup> percentile (*E95*) falls a bit less, about 50%. Thus, the positive correlation certainly softens the problem, but in no way solves it. Next, if we compare the initial and the final distributions, the average *EENS* drops by 72.36% and *E95* by 66.74%. Summing up, despite the huge improvement brought about by flexibility and seasonality, the risks around SoS continue to be extremely serious, both by past national standards and international ones.

FIGURE 2: Major adequacy metrics in 2050 (under high demand growth) in the three different settings.



## 4 CONCLUSIONS

Security of electricity supply (SoS) is a serious concern of future power generation. In a number of national systems the foreseeable development of renewable technologies and the gradual demise of nuclear and coal-fired stations can pose an added risk to security of supply. This risk can be alleviated to some extent by using the hydroelectric resources available in a flexible way. As a general rule, the power available from hydro stations depends on the operation strategies implemented by the plants' owners. In this regard, "A conservative operation will keep a minimum volume of water stored, to ensure the energy necessary to operate at full capacity in dry years; but economic optimization may lead to less conservative operation"; [2]. On the other hand, hydro plants operate in combination with other non-dispatchable technologies in a system. Consequently, a detailed analysis of the contribution of hydropower to SoS calls for taking non-dispatchable sources into account, in particular their seasonal pattern over short periods.

Here we develop a model to assess the performance of different, prospective generation parks from the viewpoint of SoS. We demonstrate it by application. At this point, instead of making assumptions on how hydro stations with reservoirs will be (or should optimally be) operated,<sup>10</sup> we draw on observed historical patterns (somehow emphasizing, as in [3], a rather physical/technical approach). We take the correlation between hydro-based power generation and peak demand into account. Specifically, we distinguish run-of-river (RoR) stations from the remainder, non-RoR hydro stations. This way we not only account for the aforementioned correlation, but for the flexible management of pump stations as well. Thus, we can assess the potential role of each particular type of hydro technology in enhancing SoS. This point is particularly important when it comes to pump stations, since the need for additional storage capacity in the future is widely recognized (not only in Spain). On the other hand, we use hourly data whenever publicly available. In particular, every month we compute the hourly seasonality attached to each type of renewable energy; this way we get a better representation of supply from renewable sources. The observed seasonal pattern is applied to the hours of maximum demand.

Our results show that flexibly managing Spanish hydro resources sizeably reduces power shortages. Yet, by itself it may not be enough to guarantee SoS during peak hours under specific configurations of the installed generation capacity. The outlook improves to some extent when the hourly seasonality of non-dispatchable generation is also considered. In general, during peak hours non-dispatchable technologies generate power above their daily averages, thus significantly contributing to SoS. This said, although the management of existing hydropower reservoirs could still be improved, [19], [23], the magnitude of our results indicates that there may be a need for (additional) demand shedding or supply increases coupled with higher storage capacity.

As [7] point out, storage projects must be assessed in the context of a changing power sector. In this regard, most stations in Spain were built when the electricity market was tightly regulated. The current liberalized market may not provide strong enough incentives to attract new investments in this area. In early 2019 the Spanish Government released the draft of the Integrated National Plan of Energy and Climate-PNIEC [24]. It surmises an increase in the installed capacity of pure pumped stations from its current level of 3,337 MW to 4,212 by 2025 and 6,837 MW by 2030. Whether the private sector will undertake these investments remains to be seen.<sup>11</sup>

Besides, as of today, none of the functions legally assigned to the power system operator (Red Eléctrica de España) implies the hydro exploitation of these generating facilities; [25]. Further, Hydrographic Confederations may set more restrictive ecological flows or limits to the rate of change of the turbined flows, which could decrease flexibility and ability to use hydropower in the operation of the power

<sup>10</sup> [7] and [21], among others, assume that utilities have perfect foresight about the day-ahead marginal electricity price when optimizing their hydro stations. [22] assume a random price of electricity, which entails the need to account for this (price) risk.

<sup>11</sup> For example, [13] warn of growing concerns regarding pumped-storage technologies as 'peak assets', because of both a diminished business case for price arbitrage (induced by the integration of subsidized renewable electricity) and the competition from alternative cheaper solutions (such as gas-fired power plants).

1  
2  
3 system, and therefore could impact its security.<sup>12</sup> According to the PNIEC, there will be regulatory changes  
4 to the operation of pure pumped stations; they would be managed by the system operator (for example, as  
5 SoS devices). Yet, as of today this legal framework remains undeveloped.

6 Regarding future research, the above analysis could be improved along several lines, both  
7 methodological and empirical (assuming the required data are publicly available). For example, solar  
8 technologies could be disaggregated into photovoltaic and thermal to account for their different  
9 charge/discharge cycles; in principle, doing so would improve the accuracy of our estimates. The empirical  
10 analysis could ideally be conducted over a longer sample period to dampen the potential impact of the dry  
11 year 2017 on the results. Beyond this, the combination of solar PV and wind parks with storage facilities  
12 can improve SoS substantially by means of technologies such as pumped hydro storage (the need to  
13 additionally invest in storage, on top of the generation facilities, makes these power systems relatively  
14 expensive in general). For example, the scenarios in [27] deploy pumped hydro (with daily-weekly storage  
15 durations) due to its technological maturity and potential in the Ontario landscape. In addition to pumped  
16 storage, [28] consider also central batteries and hydrogen storage in the future European power system.  
17 Additional storage capacity can be incorporated into our model to some extent as long as it can be  
18 interpreted like a cut in peak demand hours.  
19  
20

### 21 **Acknowledgements**

22  
23 This research is supported by the Basque Government through the BERC 2018-2021 program and by the Spanish  
24 Ministry of Economy and Competitiveness MINECO through BC3 María de Maeztu excellence accreditation  
25 MDM-2017-0714. Additionally, Luis M<sup>º</sup> Abadie and José M. Chamorro are grateful for financial support from the  
26 Spanish Ministry of Science and Innovation (ECO2015-68023). We also thank three anonymous referees for their  
27 thorough, helpful remarks and suggestions.  
28  
29  
30  
31  
32  
33  
34  
35  
36  
37  
38  
39  
40  
41  
42  
43  
44  
45  
46  
47  
48  
49  
50  
51  
52  
53  
54  
55

---

56 <sup>12</sup> [26] consider a hybrid wind/pumped-hydro system in Madeira Island (Portugal) with multiple purposes: supply water, regularize  
57 the irrigation flows, and produce electricity. They optimize the hourly operation of the pumps and turbines for a period of one day.  
58  
59

## References

- [1] European Commission (2000): "Towards a European strategy for security of energy supply". Green Paper COM (2000) 769 Final, Brussels.
- [2] European Commission (2016): Identification of Appropriate Generation and System Adequacy Standards for the Internal Electricity Market. Brussels.
- [3] Abadie L.M<sup>a</sup>, Chamorro J.M. (2019): "Physical adequacy of a power generation system: The case of Spain in the long term". *Energy* 166, 637-652.
- [4] Bailera M., Lisbona P. (2018): "Energy storage in Spain: Forecasting electricity excess and assessment of power-to-gas potential up to 2050". *Energy* 143, 900-910.
- [5] Tester J.W., Drake E.M., Driscoll M.J., Golay M.W., Peters W.A. (2005): *Sustainable Energy: Choosing Among Options*. The MIT Press, Cambridge MA.
- [6] Rodilla P., Batlle C. (2013): Security of generation supply in electricity markets. In Pérez-Arriaga I.J. (Editor) *Regulation of the Power Sector*. Springer-Verlag London.
- [7] Hino T., Lejeune A. (2012): "Pumped Storage Hydropower Developments". *Comprehensive Renewable Energy* 6, 405–434. doi:10.1016/b978-0-08-087872-0.00616-8.
- [8] Huertas-Hernando D., Farahmand H., Holttinen H., Kiviluoma J., Rinne E., Söder L., Estanqueiro A. (2017): Hydro power flexibility for power systems with variable renewable energy sources: an IEA Task 25 collaboration. *Wiley Interdisciplinary Reviews: Energy and Environment*, 6(1), e220.
- [9] Jacobson M.Z., Delucchi M.A., Cameron M.A., Frew B.A. (2015): "Low-cost solution to the grid reliability problem with 100% penetration of intermittent wind, water, and solar for all purposes". *Proceedings of the National Academy of Sciences* 112(49), 15060-15065.
- [10] Jacobson M.Z., Delucchi M.A., Bauer Z.A., Goodman S.C., Chapman W.E., Cameron M.A., Erwin J.R. (2017): "100% clean and renewable wind, water, and sunlight all-sector energy roadmaps for 139 countries of the world". *Joule* 1(1), 108-121.
- [11] Clack C.T., Qvist S.A., Apt J., Bazilian M., Brandt A.R., Caldeira K., Jaramillo P. (2017): "Evaluation of a proposal for reliable low-cost grid power with 100% wind, water, and solar". *Proceedings of the National Academy of Sciences* 114(26), 6722-6727.
- [12] Rohit A.K., Rangnekar S. (2017): "An overview of energy storage and its importance in Indian renewable energy sector: Part II – energy storage applications, benefits and market potential". *Journal of Energy Storage*, 13, 447–456. doi:10.1016/j.est.2017.07.01.
- [13] Guittet M., Capezzali M., Gaudard L., Romerio F., Vuille F., Avellan F. (2016): "Study of the drivers and asset management of pumped-storage power plants historical and geographical perspective". *Energy* 111, 560-579.
- [14] Ruppert L., Schürhuber R., List B., Lechner A., Bauer C. (2017): "An analysis of different pumped storage schemes from a technological and economic perspective". *Energy* 141, 368-379.



1  
2  
3 [15] Tarroja B., AghaKouchak A., Samuelsen S. (2016): “Quantifying climate change impacts on  
4 hydropower generation and implications on electric grid greenhouse gas emissions and operation”. Energy  
5 111, 295-305.  
6

7 [16] Zio E., Aven T. (2011): "Uncertainties in smart grids behavior and modeling: What are the  
8 risks and vulnerabilities? How to analyze them?". Energy Policy 39, 6308-6320.  
9

10 [17] UNIDO (2016): World Small Hydropower Development Report 2016. United Nations  
11 Industrial Development Organization (UNIDO), Vienna, and International Center on Small Hydro Power  
12 (ICSHP), Hangzhou.  
13

14 [18] Jain S.K., Singh V.P. (2003): Water resources systems planning and management 51.  
15 Elsevier.  
16

17 [19] Chattha N., Karki R., Fang F. (2017): Seasonal reservoir management in hydro dominant  
18 power systems to enhance availability. In 2017 IEEE Electrical Power and Energy Conference (EPEC), 1-5.  
19 IEEE.  
20

21 [20] Red Eléctrica de España (2017): Spanish Electricity System 2017 Report. Available at:  
22 <https://www.ree.es/en/statistical-data-of-spanish-electrical-system/annual-report/spanish-electricity-system-2017-report> (accessed 5/1/2019)  
23  
24

25 [21] Bregar Z. (2007): “Short-term optimization of the new Avce pumping plant and three  
26 existing hydro power plants on the Soca river in Slovenia”. Electric Power Systems Research 77,  
27 1410–1417.  
28

29 [22] Thompson M., Davison M., Rasmussen H. (2004): “Valuation and Optimal Operation of  
30 Electric Power Plants in Competitive Markets”. Operations Research 52(4), 546–562.  
31

32 [23] McPherson M., Tahseen S. (2018): “Deploying storage assets to facilitate variable renewable  
33 energy integration: The impacts of grid flexibility, renewable penetration, and market structure”. Energy  
34 145, 856-870.  
35

36 [24] Red Eléctrica de España (2014): Importancia del Equipo Generador Hidroeléctrico en la  
37 Operación del Sistema Eléctrico. Madrid.  
38

39 [25] Vieira F., Ramos H.M. (2008): “Hybrid solution and pump-storage optimization in water  
40 supply system efficiency: A case study”. Energy Policy 36, 4142–4148.  
41

42 [26] Spanish Government (2019): Plan Nacional Integrado de Energía y Clima, 2019. Available at:  
43 <https://www.miteco.gob.es/es/cambio-climatico/participacion-publica/marco-estrategico-energia-y-clima.aspx> (accessed 04/30/2019).  
44  
45

46 [27] McPherson M., Karney B. (2017): “A scenario based approach to designing electricity grids  
47 with high variable renewable energy penetrations in Ontario, Canada: Development and application of the  
48 SILVER model”. Energy 138, 185-196.  
49

50 [28] Schlachtberger D.P., Brown T., Schramm S., Greiner M. (2017): “The benefits of  
51 cooperation in a highly renewable European electricity network”. Energy 134, 469-481.  
52  
53

## Appendix

Table A1 displays the total installed capacities (in MW) of power technologies in mainland Spain and the peninsular total annual demand (in GWh). Source: [3].

|                     | 2017    | $S_1$ (demand growth: +1.36%) |         |         |         | $S_2$ (demand growth: +1.73%) |         |         |         |
|---------------------|---------|-------------------------------|---------|---------|---------|-------------------------------|---------|---------|---------|
|                     |         | 2020                          | 2030    | 2040    | 2050    | 2020                          | 2030    | 2040    | 2050    |
| Nuclear             | 7,117   | 7,117                         | 3,040   | 0       | 0       | 7,117                         | 3,040   | 0       | 0       |
| Coal                | 9,536   | 9,536                         | 6,642   | 0       | 0       | 9,536                         | 6,642   | 0       | 0       |
| Natural Gas         | 24,948  | 24,948                        | 24,948  | 24,948  | 24,948  | 24,948                        | 24,948  | 24,948  | 24,948  |
| Hydro:              | 20,331  | 20,331                        | 21,900  | 24,700  | 25,600  | 20,331                        | 23,300  | 25,900  | 28,600  |
| RoR                 | 2,104   | 2,104                         | 2,104   | 2,104   | 2,104   | 2,104                         | 2,104   | 2,104   | 2,104   |
| Non-RoR             | 18,227  | 18,227                        | 19,796  | 22,596  | 23,496  | 18,227                        | 21,196  | 23,796  | 26,496  |
| Wind                | 22,863  | 26,000                        | 28,700  | 32,100  | 35,800  | 24,500                        | 32,600  | 39,800  | 44,400  |
| Solar               | 6,730   | 16,000                        | 20,500  | 24,600  | 29,400  | 15,100                        | 20,300  | 27,300  | 39,300  |
| Cogen.              | 6,373   | 8,100                         | 9,900   | 10,800  | 11,600  | 8,100                         | 10,800  | 13,200  | 16,100  |
| Others              | 1,413   | 1,200                         | 2,800   | 3,800   | 5,300   | 1,200                         | 2,000   | 3,500   | 6,200   |
| <b>Total(MW)</b>    | 99,311  | 113,232                       | 118,430 | 120,948 | 132,648 | 110,832                       | 123,630 | 134,648 | 159,548 |
| <b>Demand (GWh)</b> | 253,082 | 263,621                       | 302,026 | 346,026 | 396,436 | 266,564                       | 316,909 | 376,762 | 447,920 |

Table A2 displays the basic statistics derived from our sample data of non-RoR stations (left block) and those resulting from 50,000 simulation runs (on the right). They are almost identical, which renders our MC-based adequacy metrics relatively reliable. In other words, this table basically serves as a cross-check of our non-RoR parameters in the simulations above. For pumped-storage stations we use an availability rate of 60.66% of their installed capacity; this is the 95<sup>th</sup> percentile of the 2015-2017 daily series.

| Month     | Estimated    |                     |        | Simulated    |                     |        |
|-----------|--------------|---------------------|--------|--------------|---------------------|--------|
|           | Mean $\mu_P$ | Volatil. $\sigma_P$ | $\rho$ | Mean $\mu_P$ | Volatil. $\sigma_P$ | $\rho$ |
| January   | 0.368        | 0.101               | 0.256  | 0.368        | 0.101               | 0.256  |
| February  | 0.404        | 0.122               | 0.381  | 0.404        | 0.122               | 0.382  |
| March     | 0.430        | 0.107               | 0.449  | 0.430        | 0.107               | 0.451  |
| April     | 0.332        | 0.138               | 0.326  | 0.332        | 0.138               | 0.326  |
| May       | 0.315        | 0.135               | 0.101  | 0.315        | 0.135               | 0.100  |
| June      | 0.254        | 0.094               | -0.012 | 0.254        | 0.094               | -0.013 |
| July      | 0.223        | 0.094               | 0.369  | 0.223        | 0.094               | 0.368  |
| August    | 0.201        | 0.077               | 0.215  | 0.201        | 0.077               | 0.216  |
| September | 0.199        | 0.069               | 0.194  | 0.199        | 0.069               | 0.193  |
| October   | 0.224        | 0.088               | 0.179  | 0.224        | 0.088               | 0.180  |
| November  | 0.233        | 0.105               | 0.152  | 0.232        | 0.105               | 0.153  |
| December  | 0.236        | 0.098               | 0.101  | 0.235        | 0.098               | 0.100  |

Table A3 shows the maximum generation potential from hydro stations (in Spanish, ‘*producibile hidrulico*’) and power demand as an approach to explaining the factor(s) behind the monthly changing correlation between the former’s load factor and the latter.

| Month     | Hydropower potential (GWh) |       |       | Power demand (GWh) |        |        |
|-----------|----------------------------|-------|-------|--------------------|--------|--------|
|           | 2015                       | 2016  | 2017  | 2015               | 2016   | 2017   |
| January   | 2,612                      | 6,024 | 1,124 | 22,694             | 21,470 | 23,109 |
| February  | 4,204                      | 4,889 | 3,802 | 21,013             | 20,848 | 19,912 |
| March     | 4,133                      | 4,603 | 2,667 | 21,184             | 21,477 | 21,128 |
| April     | 2,913                      | 6,105 | 1,546 | 18,851             | 19,931 | 18,833 |
| May       | 2,576                      | 5,483 | 1,990 | 19,832             | 19,732 | 20,242 |
| June      | 1,535                      | 2,112 | 1,074 | 20,377             | 20,247 | 21,709 |
| July      | 578                        | 915   | 557   | 23,470             | 22,235 | 22,401 |
| August    | 647                        | 367   | 253   | 20,880             | 21,464 | 21,809 |
| September | 877                        | 470   | 287   | 19,591             | 20,845 | 20,215 |
| October   | 1,503                      | 729   | 411   | 19,728             | 19,852 | 20,252 |
| November  | 1,980                      | 1,592 | 528   | 19,880             | 20,663 | 20,950 |
| December  | 1,314                      | 1,378 | 1,734 | 20,897             | 21,336 | 22,181 |

Source: Red Eltrica de Espaa (REE).

Figure A1 displays both series from Jan 2015 to Dec 2017. Hydro potential is measured along the left vertical axis; demand goes along the right one. In both cases, monthly values represent percentages, i.e. the absolute levels are divided by the yearly totals. For instance, demand in Jan 2015 accounted for 9.14% of total demand in 2015; hydro potential in the same month represented 11.31% of total potential in that year. A clear seasonal pattern arises, particularly in hydro potential, which is at its highest in winter and lowest in summer; instead, demand peaks in January and July. Overall the two (whole) series seem pretty much uncorrelated (the coefficient is -0.14); different seasonal patterns can explain this to some extent. There are wide gaps and trend mismatches in summer, but the two series comove a number of months.

FIGURE A1: Hydropower potential and power demand in mainland Spain 2015-2017.

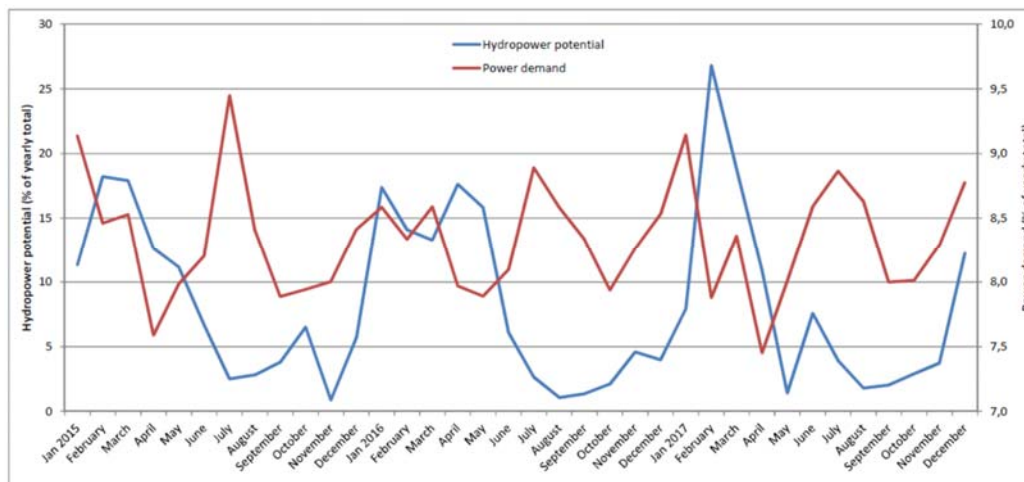


Figure A2 below displays the actual operation profile of pure pumped storage (PHES) plants in Spain. We have collected their hourly generation over the period 2014-2018, i.e. 43,824 observations. Each bar shows the number of hours when their net generation level falls between the bounds shown on the horizontal axis. Even though their aggregate installed capacity amounts to 3,337 MW, their usual net output is quite far from operation at full capacity.

FIGURE A2: Hours with positive net generation from PHES stations, 2014-2018. Source: Own elaboration on REE data.

